Sensors & Transducers, Vol. 161, Issue 12, December 2013, pp. 311-317

Sensors & Transducers

Modal and Harmonic Response Analysis of PBGA and S-N Curve Creation of Solder Joints

[1] Yu Guo, [1] Kailin Pan, [1, 2] Xin Wang, [1, 2] Tao Lu and [2] Bin Zhou

[1] School of Mechanical and Electrical Engineering, Guilin University of Electronic Technology, 1 Jinji Road, Guilin, 541004, China

[2] Science and Technology on Reliability Physics and Application of Electronic Component Laboratory, CEPREI
110 Dongguanzhuang Road, Tianhe District, Guangzhou, 510000, China

E-mail: gac_guo@foxmail.com, panklphd@gmail.com, zhoubin722@163.com

Received: 18 September 2013 /Accepted: 22 November 2013 /Published: 30 December 2013

Abstract: In recent years, with the rapid development of the microelectronics industry and the wide application of high-density packaging of electronic products, the environmental requirements for electronic products become harsh increasingly. In addition to the thermal stress, the micro-assembly device will also withstand the effects of vibration and shock with different forms, which may aggravate the elastic and plastic deformation of solder. So that increasing the accumulation of fatigue damage and even make entire electronic product failure. This paper focus on the vibration reliability of PBGA, the model test is conducted in order to ascertain the natural frequency and damping ratio, amplification coefficient, and then sine sweep test at different excitation conditions can be carried out until a solder joint become failure. The finite element model is developed by the ANSYS software. By comparing the results, the stress and strain distribution of failure joint in the first-order frequency range are attained. Finally, a numerical simulation method to obtain the curve of stress and number of the cycle to fail is developed in this paper. *Copyright © 2013 IFSA.*

Keywords: Harmonic response analysis, Modal analysis, PBGA, S-N curve.

1. Introduction

High-density electronic components are vulnerable to a variety of factors random vibration in the process of transport and using, which will cause by high cycle fatigue failure of solder joints so that make the whole PCB component failure. The increasing harsh environments of electronic products will exacerbate the plastic deformation component solder joints, which makes the rapid accumulation of fatigue damage and even the whole equipment failure. Therefore, the vibration dynamic characteristics and reliability of solder joints has become the focus of attention [1-2]. Generally, the failure of solder joints mainly caused by two main reasons: one is the low cycle thermal fatigue (thermal shock), the other is the high-cycle mechanical fatigue (such as shock, dropping and vibration loads) [3]. However, the present study on the solder joints under high cycle fatigue life prediction are involved not deep enough [4-5].

Aiming at these issues, hammering method is applied for modal test of PBGA sample. The first six order natural frequency and vibration mode are acquired. Meanwhile, the passing rate of the whole system is measured by frequency sweep mode, which provides the basis for establishment and amendment of finite element model. Based on the modal text, the first-order natural frequency is 460 Hz, so the sine sweep range is set to 431.5 Hz to 488.5 Hz. Respectively, 5 g, 10 g, 15 g excitation were applied to the system in order to measure the cycle to failure for each excitation.

After that the ANSYS software is applied to simulate the modal analysis and harmonic response analysis, so that the stress of the failure solder joint can be obtained under different excitation. By the numerical method, the S-N curve of PBGA can be fitted eventually.

2. Methodology of Test and Simulation

2.1. Test

Hammer excitation is used on modal test, the elastic hammer percussion test plate were distributed 35 points, uniformly. Two micro mass acceleration sensors were mounted on the center of the PCB board and close to the screws. The small mass sensor can minimize the effect of additional mass on the modal parameters. During in the test, the acceleration sensor generates a signal to the intelligent multi-channel data acquisition system (DASP, Analysis Tech Inc. Type: STD-128) and then obtaining mode shapes, natural frequency and damping ratio. To verify the reliability of vibration and the transfer characteristic fixture of the sample, the sine sweep experiments at different excitation conditions are conducted on the sample, and the sweep range is around the first-order natural frequency.

2.2. Simulation

2.2.1. Modeling

In order to simplify the calculation process, half of the solid model is established according to the symmetry of BGA and the PCB. The BGA component model is set up as shown in Fig. 1. Table 1 illustrates material parameters of each part on PCB component and material parameters of each components for BGA defined in ANSYS 14.

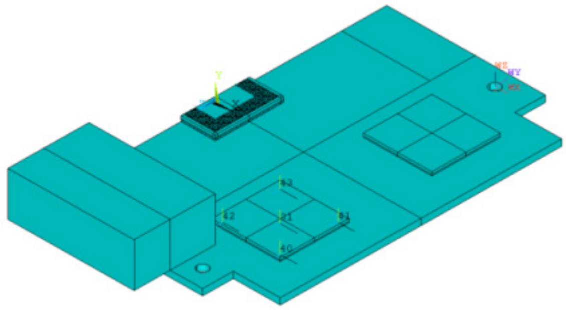

Fig. 1. Quarter of finite element model.

Table 1. Material properties of PCB component.

Construction	E (GPa)	G (GPa)	ν	ρ (kg/m³)
Solder joints	49.4	/	0.4	7531
Copper pad	120	/	0.35	8940
Solder mask	5.00	/	0.467	1000
Substrate	E_x, E_y: 16.8 E_z: 7.40	G_{xz}, G_{yz}: 7.59 G_{xy}: 3.31	ν_{xz}, ν_{yz}: 0.39 ν_{xy}: 0.11	1910
Die	131	/	0.23	2330
Plastic encapsulant	28.0	/	0.35	1890
PCB	E_x, E_y: 18.48 E_z: 8.14	G_{xz}, G_{yz}: 8.35 G_{xy}: 3.64	ν_{xz}, ν_{yz}: 0.39 ν_{xy}: 0.11	1910

Note: E-Elasticity modulus; G-Shear modulus; ν-Poisson's ratio; ρ-Density.

2.2.2. Meshing and Boundary Conditions

Meshing quality determines the accuracy of the result directly. In order to get a relatively accurate calculated result, the main observation components adopt fine meshing method while the rest of the non-main parts adopt smart meshing of system kernel. The method can ensure the meshing quality, improve the operation efficiency and reduce the workload [6].

For the BGA on the PCB, mapped meshing and sweep meshing method are used. The BGA in the middle uses penetrating mapped meshing method. All the internal structures of BGA are meshed regularly and the ultra-thin body units such as the solder mask, copper pad can also be well meshed, as shown in Fig. 2. In order to mapped and sweep conveniently, the PCB and I/O interface have been divided into several parts in the modeling.

The only effective "load" is zero displacement constraints in typical modal analysis. Therefore, only zero displacement constraints are applied in PCB component screw holes respectively. For symmetric cross section, symmetry constraints are applied as constraint conditions.

3. Results and Discussion

3.1. Results Analysis of Modal

3.1.1. Experimental Results Analysis of Modal

Table 2 shows the test results of the first six orders natural frequency and damping ratio respectively. From the table, the first-order main vibration mode presents longitudinal bending modal, the bending vibration mainly towards the positive direction of Z axis, the largest amplitude appears near the center, and there is no obvious bending deformation on both sides of the screw fixed place and its nearby areas. With the increase of modal order, modal vibration mode becomes more complex, and presents the composite bend torsion modal, the degree of bend and torsion becomes more complex, and solder joints on the component are easier affected by the tensile stress and tensile stress. At the same time, thus brings challenges to the layout design of component. Therefore, electronic products which always work under high frequency vibration environment need to accurately measure high-order modal mode of vibration specially, to avoid vibration sensitive element arranges in bending and twisting modal areas [7].

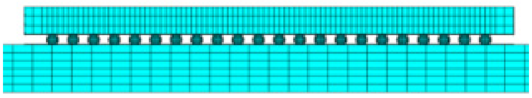

(a) Cross section of BGA meshing;

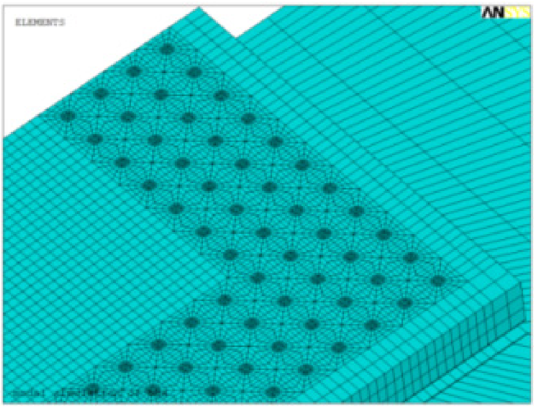

(b) Drawing of partial enlargement

Fig. 2. Meshing model of BGA component.

Table 2. Modal frequency and modal damping.

Select Shape	Frequency (or Time)	Damping	Units	Damping (%)
1	460	3.56	Hz	0.554
2	633	3.51	Hz	0.489
3	787	4.77	Hz	0.516
4	1.05E+03	9.5	Hz	0.825
5	1.28E+03	10.4	Hz	0.753
6	1.54E+03	14.4	Hz	0.896

3.1.2. The Contrast Analysis for the Experimental Results and Simulation Results

Table 3 shows the comparison between the modal test and finite element simulation for the first seven orders natural frequency, Table 4 shows the comparison between the experiment and simulation for the first two order modes of vibration. From the above two tables, the first two order modes of the modal are characterized by the longitudinal bending towards the vertical of board face, while the third-order mode is characterized by transverse bending vibration, each order modal shows good consistency, first-order natural frequency also fits well. The 6.25 % of the maximum error rate between the simulation results and test results is acceptable, thereby verifying the validity of the finite element model and simulation method, laying a foundation for the follow-up study of modal characteristics under more fixed constraints.

Table 3. Comparison between the first two frequencies of experiment and simulation.

Modes order	Test results (Hz)	Simulation results (Hz)	Error	Error rate
1	460	472.8	12.8	2.26 %
2	633	663.2	30.2	4.09 %
3	787	807.5	30.5	3.41 %
4	1050	1125	75	6.25 %
5	1280	1347.4	67.4	4.71 %
6	1540	1591.5	51.5	3.05 %

Table 4. Comparison between the first three vibration mode of experiment and simulation.

Or-der	Test results	Simulation results	Vibration mode
1	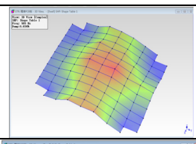	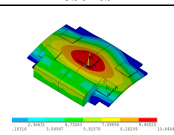	1-st order longitu-dinal bending
2	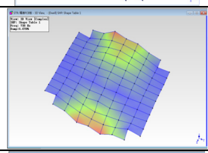	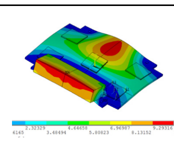	2-st order longitu-dinal bending
3	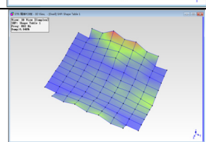	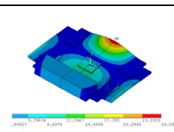	1-st order transverse bending
4	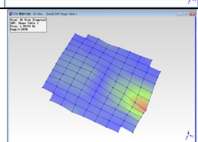	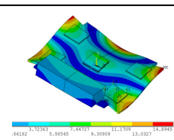	Bending-torsion complex
5	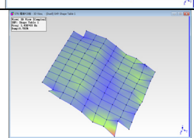	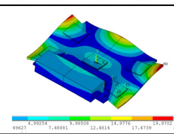	Bending-torsion complex
6	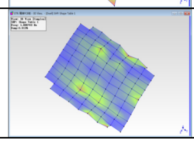	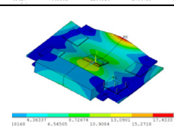	Bending-torsion complex

The analysis suggests that the cause of a certain error in the first order frequency has something to do with the finite element meshing, simplified material structure and error during the test. Error rate increases with the increase of frequency order number, because the finite element analysis deals with the high frequency components and noise interference of the model ideally. At the same time, the differences on the constraint conditions between simulation analysis and modal test may also lead to a certain error, such as screw clamped constraints. There is always a slight translation and rotation under screw constraints of the modal test actually, while finite element simulation uses full freedoms constraint and assumes the translational and rotational degrees of freedom are zero at solid fulcrum [8].

3.2. Results Analysis of Harmonic Response

3.2.1. Sine Vibration Test

To verify the transfer characteristics and dynamic characteristics of fixture itself, to avoid test system resonance caused by too low inherent frequency of fixture, at the same time, to quickly analysis the deformation of PCB components caused by each order frequency and the relationship between maximum deformation of PCB components and input incentive load, by using the sine sweep vibration method, the initial vibration test under different input load is applied for vibration fixture itself and the PCB components respectively. Meanwhile, the obtained transfer rate and amplification coefficient provide the basis for the correction of further finite element model.

After the sensors arranging in different positions respectively and applying sine excitation, the maximum frequency corresponded to amplification coefficients are shown in Table 5.

Table 5. Vibration amplification coefficient and frequency points under different excitations.

Test Mode	Frequency point at maximum value	Amplification coefficient
5g excitation (between PCB and fixture)	568.8	74.93
5g excitation (between PCB and component)	563.7	1.24
10g excitation (between PCB and fixture)	565	55.75
10g excitation (between PCB and component)	563.7	1.25

3.2.2. Stress-Strain Analysis of Dangerous Point under Different Excitations

Fig. 3 shows the stress distribution of dangerous point with the excitation acceleration of 15G. It illustrates that the maximum equivalent stress occurs at the corner of the outermost solder joint of PBGA which is in the middle of PCB. The value of the maximum equivalent stress is 41.3 MPa and the stress concentration area is located at the soldering interface between PBGA and solder joint. Solder joints at outer side of the PBGA is of larger stress while the inner ones are of lower stress. The solder joints of PBGAs which are located at the sides of the PCB and near the set screw also have lower stress. From the forgoing, it can be concluded that the bending deformation of PCB assemblies is likely appeared periodically in the direction of the perpendicular of the PCB under the vibration shock.

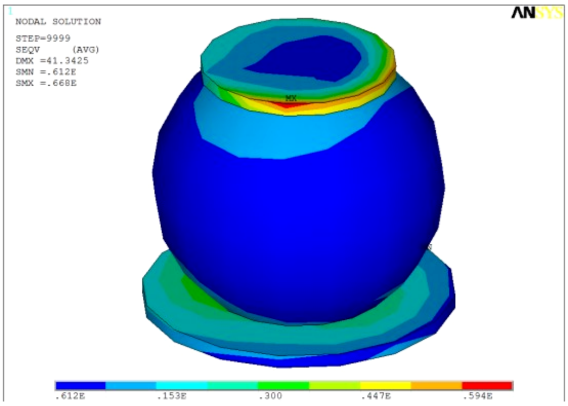

(a) Stress distribution in solder joint.

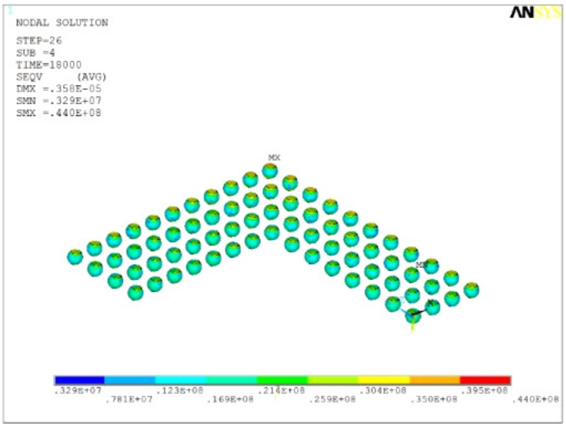

(b) Solder joints of BGA.

Fig. 3. Stress distribution of dangerous point with the excitation acceleration of 15G.

This kind of bending deformation can result in the periodic stress loaded to the solder joints. Due to the corner of outermost solder joint of the PBGA shown in Fig. 3 has the maximum deformation, thus, the equivalent stress of the solder joints largest. The amplitude of solder joints and PCB at dangerous frequency is demonstrated in Fig. 4. Based on stress failure criterion, the solder joint that has the maximum deformation shown in Fig. 3 is specified as the key solder joint. However, the position of crack initiation and the direction of crack propagation cannot be determined by the maximum stress distribution. In addition, it can be inferred that the solder mask defined pads between solder joints and PBGA are easy to cause stress concentration in the condition of random vibration load, while the non-solder mask defined pads between solder joints and PCB are beneficial to release the stress. Hence, the maximum stress is located at the interface between solder joints and BGA. Fig. 5 shows the curve of frequency-amplitude response and frequency-phase response respectively.

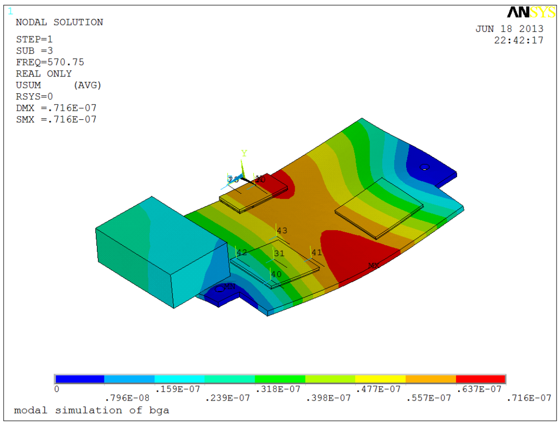

(a) Amplitude of one-half of the PCB.

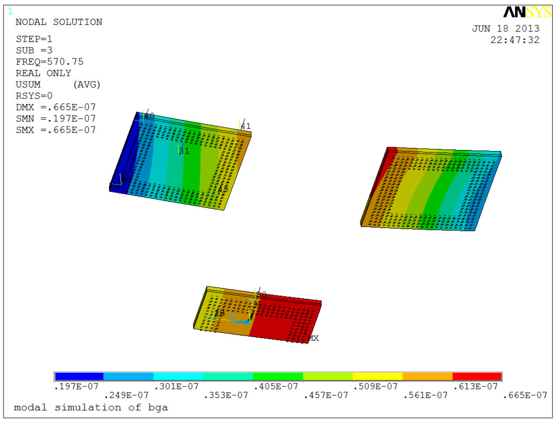

(b) Amplitude of the BGAs on one-half of PCB.

Fig. 4. Amplitude of solder joints and PCB at dangerous frequency.

3.3. The Creation of S-N Curve Based on the Simulation Result of Harmonic Response Analysis

Von Mises equivalent stress is regarded as an accurate one in life prediction model [9]. This study loads different excitations on PCB by using finite element simulation to implement harmonic response analysis, and then extracts the equivalent stress of every single node in the dangerous area from the simulation results. Finally, the mass mean equivalent stresses is taken as the stress of S-N curve. The equivalent stress of elements in the dangerous area is listed in Table 6.

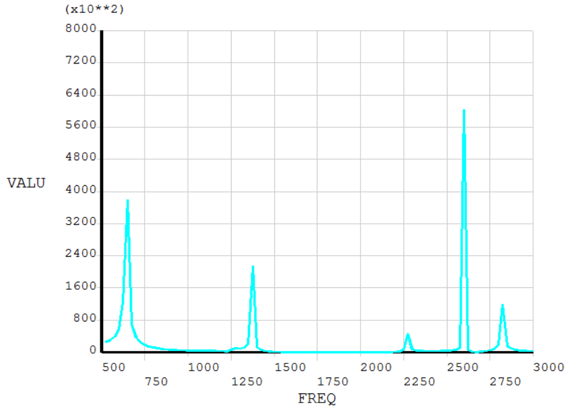

(a) Frequency-amplitude response.

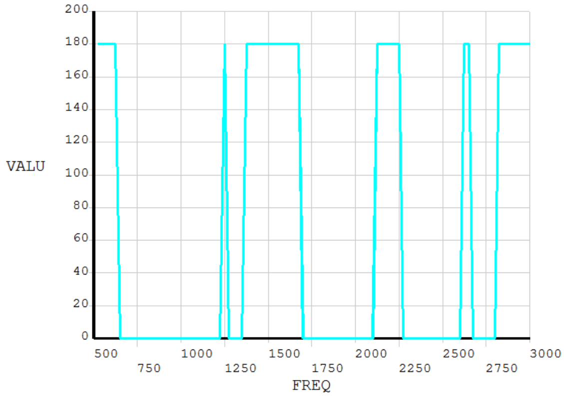

(b) Frequency-phase response.

Fig. 5. Curve of frequency-amplitude response and frequency-phase response.

Table 6. Equivalent stress of elements at dangerous area under different excitations.

5G		10G		15G	
Element number	**Stress (MPa)**	**Element number**	**Stress (MPa)**	**Element number**	**Stress (MPa)**
169838	11.3	169835	22.5	169935	33.8
169929	11.8	169932	22.6	170027	30.5
169912	12.1	169915	22.3	169920	29.7
169932	12	169939	21.5	169939	29
169750	11.7	169756	21.7	169756	29.4
169755	11.5	169762	21.2	169762	29.2
169971	11.7	169973	21.3	169974	28.9
169932	11.2	169937	20.9	169937	28.6

Compared to the height of the BGA, the diameter of the solder ball is relatively smaller. Therefore, mass mean stress method is adopted for this area. As Formula (1) revealed, σ_{avg} stands for the overall average equivalent stress value, V_ε stands for the volume of each element, and σ stands for the equivalent stress of each element.

$$\sigma_{avg} = \frac{\sum \sigma \cdot V_\varepsilon}{\sum V_\varepsilon} \quad (1)$$

Bringing the equivalent stress of each node in the dangerous area listed in Table 7 into Formula (1), the results are worked out shown in the table below.

Table 7. σ_{avg} value corresponding to different excitation.

Excitation / Result	5G	10G	15G
σ_{avg}	11.66	21.75	29.9

The failure time of sinusoidal vibration which is obtained from the experiment are transformed into failure cycle N by using Formula (2). In this formula, denominator stands for the range of sinusoidal sweep frequency, numerator stands for the half-power point, and *t* stands for the failure time. With different excitations, the failure time of sinusoidal sweep frequency vibration experiment and the counted times of failure cycle are given in the Table 8.

Table 8. Failure time of solder joint under different excitations.

Excitation	5G	10G	15G
Failure time	33h	7.2h	0.95h
N_f	7000000	1500000	202400

$$N_f = \left(\frac{3.59 \times 2}{488 - 431}\right) \cdot t \cdot 460 \quad (2)$$

According to Formula (3), the mass mean stress is fitted with the failure cycle times of failure solder balls under different excitation conditions. Then the preliminary S-N curve can be acquired as Fig. 6 and Formula (4) demonstrated.

$$\sigma_a = \sigma' f (2N_f)^b \quad (3)$$

In Formula (3), σ_a stands for stress amplitude. $\sigma' f$ stands for the failure strength coefficient. b stands for the failure strength index. And N_f stands for the failure cycle times. According to the fitting curve given in the Fig. 6, $\sigma' f$ can be 768.1 MPa and the failure strength index b can be -0.25 for the solder.

$$y = 768.1 \cdot x^{-0.26} \quad (4)$$

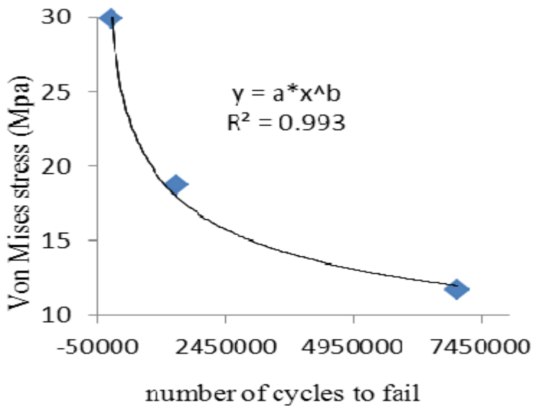

Fig. 6. S-N curves of the solder joints.

4. Conclusions

In order to explore the dynamics of PBGA, the model test and sine sweep test is conducted on PBGA sample, firstly. Hammering method is applied for modal test of PBGA sample and the first six orders natural frequency is 460 Hz, 633 Hz, 787 Hz, 1050 Hz, and 1280 Hz, respectively. The failure cycles which measured by sine experiment under the excitation of 5 g, 10 g, 15 g are 7000000, 1500000, 202400 respectively. Also, based on the comparison between modal analysis and test results, it shows that the first two order modes of the modal are characterized by the longitudinal bending towards the vertical of the board, while the third-order mode is characterized by transverse bending vibration, each order modal shows good consistency, first-order natural frequency also fits well. From the harmonic response simulation, the maximum equivalent stress occurs at the corner of the outermost solder joint of PBGA which is in the middle of PCB. The value of the maximum equivalent stress is 34.1 MPa and the stress concentration area is located at the soldering interface between PBGA and solder joint. Solder joints at outer side of the PBGA is of larger stress while the inner ones are of lower stress. Mass mean stress of different excitation and the corresponding equivalent stress are obtained based on the simulation analysis, which is used for fitting the S-N curve.

Acknowledgements

This work is supported by Guangxi Natural Science Fund for Distinguished Young (Grant No.2012jjFAG0004), the Major Project of Guangxi

Natural Science Foundation (Grant No. 210GXNSFD013039) and Innovation Project of Guangxi Graduate Education (Grant No. YCSZ2013066).

References

[1]. Zhou Y., Al-Bassyiouni M., Dasgupta A., Harmonic and random vibration durability of SAC305 and Sn37Pb solder alloys, *IEEE Tran.s Compon.. Pack.. Technol.*, 33, 2, June 2010.

[2]. Chen Y.S., *et al.*, Combining vibration test with finite element analysis for the fatigue life estimation of PBGA components, *Microelectronics Reliability,* 48, 2008, pp. 638–644.

[3]. Che F. X., Pang John H. L., Vibration reliability test and finite element analysis for flip chip solder joints, *Microelectronics Reliability,* 49, 2009, pp. 754–760.

[4]. Yang Q. J., Pang H. L. J., Wang Z. P., Lim G. H., Yap F. F., Lin R. M., Vibration reliability characterization of PBGA assembly, *Microelectronics Reliability,* 16, 2000, pp. 1097–1107.

[5]. Pitarresi J. M., Akanda A., Random vibration response of a surface mounted lead/solder joint, in *Proceedings of the ASME International Electronics Packaging Conference,* Binghamton, NY, 1, September 1993, pp. 207–217.

[6]. Barker D. B., Chen Y. S., Dasgupta A., Estimating the vibration fatigue life of quad leaded surface mount components, *J. Electron. Packag.,* 115, 1993, pp. 195-200.

[7]. Pitarresi J. M., Akanda A., Random vibration response of a surface mount lead/solder joint, *Adv Electron Packag*, EEP-4-1, 1993, pp. 207-215.

[8]. Wong T. L., Stevens K. K., Wang G., Experimental modal analysis and dynamic response prediction of PC boards with surface mount electronic components, *J Electron Package,* 113, 1991, pp. 244-249.

[9]. Da Yu, *et al.,* High-cycle fatigue life prediction for Pb-free BGA under random vibration loading, *Microelectronics Reliability,* 51, 2011, pp. 649–656.